MICROCOPY RESOLUTION TEST CHART

NATIONAL BUREAU OF STANDARDS-1963-A

DNA-TR-86-34

PIEZOELECTRIC RESPONSE OF POLYVINYLIDENE FLUORIDE TO COMBINED COMPRESSION AND SHEAR

John B. Aidun
SRI International
333 Ravenswood Avenue
Menlo Park, CA 94025-3434

31 December 1985

Technical Report

DTIC
ELECTE
OCT 9 1986
S D
B

Prepared for
    Director
    DEFENSE NUCLEAR AGENCY
    Washington, DC 20305-1000

86 10 9 131

DISTRIBUTION LIST UPDATE

This mailer is provided to enable DNA to maintain current distribution lists for reports. We would appreciate your providing the requested information.

☐ Add the individual listed to your distribution list.

☐ Delete the cited organization/individual.

☐ Change of address.

NAME: _____

ORGANIZATION: _____

OLD ADDRESS	CURRENT ADDRESS
_____	_____
_____	_____
_____	_____

TELEPHONE NUMBER: ( ) _____

SUBJECT AREA(s) OF INTEREST:

_____	_____
_____	_____
_____	_____

DNA OR OTHER GOVERNMENT CONTRACT NUMBER: _____

CERTIFICATION OF NEED-TO-KNOW BY GOVERNMENT SPONSOR (if other than DNA):

SPONSORING ORGANIZATION: _____

CONTRACTING OFFICER OR REPRESENTATIVE: _____

SIGNATURE: _____

Director
Defense Nuclear Agency
ATTN: STTI
Washington, DC 20305-1000

REPORT DOCUMENTATION PAGE

1a. REPORT SECURITY CLASSIFICATION UNCLASSIFIED			1b. RESTRICTIVE MARKINGS			
2a. SECURITY CLASSIFICATION AUTHORITY N/A since Unclassified			3. DISTRIBUTION / AVAILABILITY OF REPORT Approved for public release; distribution is unlimited.			
2b. DECLASSIFICATION / DOWNGRADING SCHEDULE N/A since Unclassified						
4. PERFORMING ORGANIZATION REPORT NUMBER(S) PYU-7773			5. MONITORING ORGANIZATION REPORT NUMBER(S) DNA-TR-86-34			
6a. NAME OF PERFORMING ORGANIZATION SRI INTERNATIONAL	6b. OFFICE SYMBOL (If applicable)		7a. NAME OF MONITORING ORGANIZATION Director Defense Nuclear Agency			
6c. ADDRESS (City, State, and ZIP Code) 333 Ravenswood Avenue Menlo Park CA 94025 - 3434			7b. ADDRESS (City, State, and ZIP Code) Washington, DC 20305-1000			
8a. NAME OF FUNDING / SPONSORING ORGANIZATION	8b. OFFICE SYMBOL (If applicable)		9. PROCUREMENT INSTRUMENT IDENTIFICATION NUMBER DNA 001-84-C-0377			
8c. ADDRESS (City, State, and ZIP Code)			10. SOURCE OF FUNDING NUMBERS			

			PROGRAM ELEMENT NO 62715H	PROJECT NO RJ	TASK NO RD	WORK UNIT ACCESSION NO DH008575

11. TITLE (Include Security Classification)   PIEZOELECTRIC RESPONSE OF POLYVINYLIDENE FLUORIDE TO COMBINED COMPRESSION AND SHEAR

12. PERSONAL AUTHOR(S)
Aidun, John B

13a. TYPE OF REPORT Technical Report	13b. TIME COVERED FROM 840701 TO 851231	14. DATE OF REPORT (Year, Month, Day) 851231	15. PAGE COUNT 38

16. SUPPLEMENTARY NOTATION   This work was sponsored by the Defense Nuclear Agency under RDT&E RMC Code B3450844662 RJ RD 10010 25904D.

17.	COSATI CODES		18. SUBJECT TERMS (Continue on reverse if necessary and identify by block number)	
FIELD	GROUP	SUB-GROUP	Piezoelectric Measurements	PVDF
20	05		Stress Gage	PVF_2
22	02		Dynamic Loading	Polyvinylidene Fluoride

19. ABSTRACT (Continue on reverse if necessary and identify by block number)

In this project we performed inclined-impact wave propagation experiments to assess the shear-stress sensitivity of the piezoelectric polyvinylidene fluoride (PVDF) sensing element of the National Bureau of Standards (NBS) soil stress gage. No sensitivity to shear stress was expected. However, because of deficiencies in the general understanding of the piezoelectric response of PVDF, especially under large stresses and strains, direct measurements were necessary to confirm this expectation. In a set of four plate-impact experiments, we investigated one combination of stress wave amplitudes: a 4.5-kbar (450 MPa) compressive stress and a 0.22-kbar (22 MPa) shear stress. The results are ambiguous and inconclusive. However, we could detect no piezoelectric sensitivity of the PVDF to in-plane shear stress. From this observation, we make a tentative estimate that the piezoelectric sensitivity of the NBS PVDF sensing element to in-plane shear stress is less than

20. DISTRIBUTION / AVAILABILITY OF ABSTRACT ☐ UNCLASSIFIED/UNLIMITED ☒ SAME AS RPT ☐ DTIC USERS	21. ABSTRACT SECURITY CLASSIFICATION UNCLASSIFIED	
22a. NAME OF RESPONSIBLE INDIVIDUAL Betty L. Fox	22b. TELEPHONE (Include Area Code) (202) 325 7042	22c. OFFICE SYMBOL DNA/STTI

DD FORM 1473, 84 MAR   83 APR edition may be used until exhausted   SECURITY CLASSIFICATION OF THIS PAGE
All other editions are obsolete

19. ABSTRACT (Continued)

0.27 times its sensitivity to hydrostatic compression. We discuss the uncertainties in the experiments and review the outstanding questions concerning the piezoelectric response of PVDF. We suggest two experimental methods that could usefully augment the observations that can be made from inclined-impact experiments.

PREFACE

CONVERSION TABLE

Conversion factors for U.S. Customary to metric (SI) units of measurement

MULTIPLY ⟶ BY ⟶ TO GET
TO GET ⟵ BY ⟵ DIVIDE
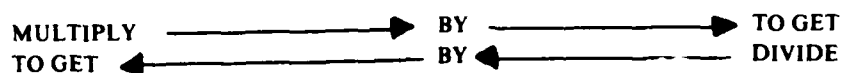
angstrom	1.000 000 X E -10	meters (m)
atmosphere (normal)	1 013 25 X E +2	kilo pascal (kPa)
bar	1.000 000 X E +2	kilo pascal (kPa)
barn	1.000 000 X E -28	meter^2 (m^2)
British thermal unit (thermochemical)	1.054 350 X E +3	joule (J)
calorie (thermochemical)	4.184 000	joule (J)
cal (thermochemical)/cm^2	4.184 000 X E -2	mega joule/m^2 (MJ/m^2)
curie	3.700 000 X E +1	*giga becquerel (GBq)
degree (angle)	1.745 329 X E -2	radian (rad)
degree Fahrenheit	$t_K = (t°f + 459.67)/1.8$	degree kelvin (K)
electron volt	1.602 19 X E -19	joule (J)
erg	1.000 000 X E -7	joule (J)
erg/second	1.000 000 X E -7	watt (W)
foot	3.048 000 X E -1	meter (m)
foot-pound-force	1.355 818	joule (J)
gallon (U S liquid)	3 785 412 X E -3	meter^3 (m^3)
inch	2 540 000 X E -2	meter (m)
jerk	1 000 000 X E +9	joule (J)
joule/kilogram (J/kg) (radiation dose absorbed)	1.000 000	Gray (Gy)
kilotons	4 183	terajoules
kip (1000 lbf)	4.448 222 X E +3	newton (N)
kip/inch^2 (ksi)	6 894 757 X E +3	kilo pascal (kPa)
ktap	1 000 000 X E +2	newton-second/m^2 (N-s/m^2)
micron	1 000 000 X E -6	meter (m)
mil	2 540 000 X E -5	meter (m)
mile (international)	1.609 344 X E +3	meter (m)
ounce	2 834 952 X E -2	kilogram (kg)
pound-force (lbs avoirdupois)	4.448 222	newton (N)
pound-force inch	1.129 848 X E -1	newton-meter (N·m)
pound-force/inch	1 751 268 X E +2	newton/meter (N/m)
pound-force/foot^2	4.788 026 X E -2	kilo pascal (kPa)
pound-force/inch^2 (psi)	6 894 757	kilo pascal (kPa)
pound-mass (lbm avoirdupois)	4 535 924 X E -1	kilogram (kg)
pound-mass-foot^2 (moment of inertia)	4 214 011 X E -2	kilogram-meter^2 (kg·m^2)
pound-mass/foot^3	1 601 846 X E +1	kilogram/meter^3 (kg/m^3)
rad (radiation dose absorbed)	1.000 000 X E -2	**Gray (Gy)
roentgen	2 579 760 X E -4	coulomb/kilogram (C/kg)
shake	1 000 000 X E -8	second (s)
slug	1.459 390 X E +1	kilogram (kg)
torr (mm Hg, 0° C)	1.333 22 X E -1	kilo pascal (kPa)

*The becquerel (Bq) is the SI unit of radioactivity; 1 Bq = 1 event/s.
**The Gray (Gy) is the SI unit of absorbed radiation.

TABLE OF CONTENTS

Section   Page

LIST OF ILLUSTRATIONS

SECTION 1

INTRODUCTION

This report presents the results of plate-impact experiments performed by SRI International to assess the shear-stress sensitivity of the piezoelectric sensing element of a stress gage. This gage was developed by Dr. A. Bur and coworkers[1,2] at the National Bureau of Standards (NBS). The sensing element in the NBS stress gage is a double layer of the thin, polymer film, polyvinylidene fluoride (PVDF). The performance of this gage for measuring dynamic stresses in soil has been evaluated both in the laboratory and in the field.[3,4] Because those tests focused on the sensitivity of the NBS gage to normal stress, they could not provide information on the gage's sensitivity to dynamically applied shear stress.

Although there has been considerable research on the piezoelectric and mechanical properties of PVDF over the past twenty years (see, for example, reference 5), the source of its piezoelectric sensitivity is not well understood. No single model of the behavior of PVDF can be relied on to predict the shear stress sensitivity of the film used in the NBS gage. Nor can we estimate its response to shear stress by assuming that the piezoelectric behavior of the bulk film can be described by a coefficient matrix relating stress or strain to change in polarization. Such a description is adequate for many applications of single crystals that exhibit primary* piezoelectric sensitivity. The practical problem in describing the film in an analogous manner is that insufficient laboratory measurements have been performed to determine all the coefficients of an effective piezoelectric matrix of the bulk material. More important, a description of this form would probably be inaccurate for describing secondary piezoelectric behavior.

Effective field operation of a stress gage requires that its signal, which is a scalar function of time, can be unambiguously related to one component of the free-field stress, which is a tensor function of time. The stress component the NBS gage is designed to measure is the normal stress applied to the face of the gage. The small aspect ratio of the NBS gage (0.024 thickness-to-diameter) minimizes its perturbation to the stress field and restricts its sensitivity to the three components of stress that develop on the face of the gage.[3] Thus, for effective operation, we must be able to account for the influence of the two components of shear stress applied to the face of the gage on its response. If PVDF has no piezoelectric sensitivity to in-plane shear stress, the response of the NBS gage depends only on the normal stress applied on its face, and no explicit account would need to be made of coexisting shear stresses.

Based on the model of PVDF used by Bur in developing the NBS gage[6] and the general view expressed in the literature, we did not expect the PVDF to exhibit any piezoelectric sensitivity to in-plane shear stresses. Owing to the deficiencies in the general understanding of PVDF mentioned above, we undertook to perform direct measurements to confirm the absence of piezoelectric sensitivity of the NBS gage's sensing element to shear stresses applied in the plane of the PVDF film

---

* Primary piezoelectricity refers to stress-induced changes in polarization. This is distinguished from secondary piezoelectricity, in which a change in polarization results from strain-induced redistribution of free charge or permanent dipoles

We performed a set of four plate-impact experiments to assess the shear sensitivity of the PVDF sensing element to combined loading by a longitudinal and a shear stress wave. We investigated one combination of amplitudes of compressive stress and shear stress in these experiments. The compressive stress was nominally 4.5 kbar (450 MPa). Under this compression, no piezoelectric sensitivity of the PVDF sensing element to a 0.22-kbar (22 MPa) in-plane shear stress was detectable in our experiments. From this observation we estimate that the piezoelectric sensitivity of the NBS PVDF sensing element to in-plane shear stress is less than 0.27 times its sensitivity to hydrostatic compression. However, the records obtained in our experiments contain much noise, and their interpretation is ambiguous.

We have also briefly examined the feasibility of two other methods for determining whether PVDF is sensitive to shear stress. First, the SRI Hopkinson torsion bar might be used to apply dynamic shear loads of millisecond duration to the specimen rather than the short, microsecond duration pulses applied in the gas gun experiments. Second, the nonzero coefficients of the effective piezoelectric matrix of PVDF film under zero confining stress could be identified following established methods of applying electric fields to exercise the inverse piezoelectric effect in the material. This coefficient matrix would provide qualitative information: the stress or strain components that change the polarization of PVDF film under zero confining stress should also change it under nonzero confining stresses. These possibilities are discussed among the recommendations in Section 6.

SECTION 2

THE PVDF SENSING ELEMENT

PVDF is a semicrystalline polymer film with a crystalline fraction of nominally 50%. Three structural phases of PVDF crystallites have been identified.[5] Phase I (beta-phase) has orthorhombic m2m symmetry[5] (the two-fold axis is in the plane of a crystal lamella along the crystallographic b-axis). Oriented samples of Phase I PVDF are produced by stretching material crystallized from melt. Stretching tends to align the lamellae of crystallites with the plane of the film. A film that is stretched along only one direction, taken to be the x_1-direction, is called uniaxially oriented PVDF. A film that is stretched along both the x_1- and x_2-directions is called biaxially oriented. The x_3-axis of the reference coordinate system is normal to the plane of the film.

Biaxially or uniaxially oriented Phase I PVDF that is subjected to a strong electric field of the order of MV/cm along the x_3-direction becomes permanently polarized in this direction. This treatment, called poling, produces a strong piezoelectric sensitivity to normal stress in the x_3-direction. The effective piezoelectric stress coefficient (e-constant) of PVDF film relating normal strain to change in polarization along the x_3-direction is estimated to be approximately equal to the analogous coefficient of an X-cut quartz single crystal. Because the compressibility of PVDF film is much larger than that of quartz, the corresponding effective piezoelectric strain coefficient (d-constant), which relates normal stress to change in polarization, is of the order of tens of pC/N, compared to 2.25 pC/N for the analogous coefficient of an X-cut quartz single crystal.

PVDF also exhibits a pyroelectric sensitivity. This effect should be present in impact experiments, which produce an adiabatic temperature rise in the material given by

$$\left(\frac{\partial T}{\partial P} \right)_S = \frac{\alpha T}{\rho C_P} \tag{1}$$

where T is temperature, P is pressure, subscript S denotes constant entropy, α is the coefficient of thermal expansion, ρ is density, and C_P is specific heat. The fractional contribution to the change in polarization from the pyroelectric response in the impact experiments is given by

$$\frac{\lambda}{d} \left(\frac{\partial T}{\partial P} \right)_S \tag{2}$$

where λ is the pyroelectric coefficient, relating changes in temperature to changes in polarization. DeReggi and coworkers[7] take the d-constant in Eq. (2) to be d_h the effective hydrostatic d-constant, which relates a purely hydrostatic stress to the change in the polarization component P_3, and they estimate the fractional contribution of the pyroelectric response to the polarization as 8%.

Based on the symmetry of Phase I PVDF, the d-constant matrix for a single crystal has this form:

3

$$d_{ij} = \begin{bmatrix} 0 & 0 & 0 & 0 & 0 & d_{16} \\ d_{21} & d_{22} & d_{23} & 0 & 0 & 0 \\ 0 & 0 & 0 & d_{34} & 0 & 0 \end{bmatrix} \tag{3}$$

Polarization arising from primary piezoelectricity in linear elastic single crystals is related to applied stress by

$$\vec{P} = \mathbf{d} \, \vec{\sigma} \tag{4}$$

If the piezoelectric behavior of PVDF film were produced in the same manner as in single crystals, the zero elements of an effective d-constant matrix could preclude any piezoelectric sensitivity to in-plane shear stresses. However, the macroscopic symmetry of PVDF film has not been determined conclusively.

Two additional points apply. First, because of the large compressibility of PVDF, arguments based on the symmetry of the material at low stresses may not apply at the high stresses that the NBS gage is expected to measure. Finite strains under such stresses may effectively alter the macroscopic symmetry of the film. Second, a significant portion of the piezoelectric response of PVDF appears to arise from secondary piezoelectricity: the reorientation of the dipolar chain molecules within crystallites and the redistribution of crystallites and free charge within the film resulting from deformation. According to the model for PVDF[6] referred to by Bur in developing the NBS gage, these effects occur with no variation of the strength of the dipoles within the film, unlike the behavior of a stressed, piezoelectric single crystal. The symmetry of a material does not constrain the relation between applied stresses and resulting secondary piezoelectric changes in polarization. To the extent that the piezoelectric response of PVDF is secondary, arguments based on symmetry for the sensitivity of its response to particular components of stress are inapplicable.

The sensing element of the NBS gage, shown in Figure 1, comprises two layers of PVDF film, each approximately 12-μm thick. Electrodes are vapor-deposited onto each side of the circular 0.5-cm-diameter sensitized area in the center of each 2.54-cm-diameter film. The two layers are bonded together by a layer of epoxy. The total thickness of the element is nominally 50 μm. The two layers of PVDF are oriented so that the sense of the permanent polarization normal to each of the film layers are opposite one another. The two electrodes in the interior of the element are both high potential electrodes, joined electrically by a common lead. The two electrodes on the exterior faces of the element are both low potential electrodes, also joined electrically by another common lead. The leads from the electrodes reach along a radius of the films, joining to a coaxial connector.

In the complete gage package, a small thermocouple is placed between the layers of PVDF near the central sensitized area for monitoring temperature changes produced by heat flowing from the surroundings. This thermocouple was omitted from the sensing elements used in our experiments. Additionally, for all the incline-impact experiments, the exterior electrodes of each of the PVDF sensing elements were extended to cover the entire surface to provide a uniform frictional character.

Epoxy
and High
Potential
Leads

Low Potential
Electrode

0.5 cm

Active Areas

~ 12 µm

~ 50 µm

High Potential
Electrodes

Low Potential
Electrode

Biaxially Oriented
PVDF Film

(a) Cross Section

Active Area

Coaxial Cable
Connector

Low Potential
Electrical
Lead (On
Surface)

0.5 cm

2.54 cm
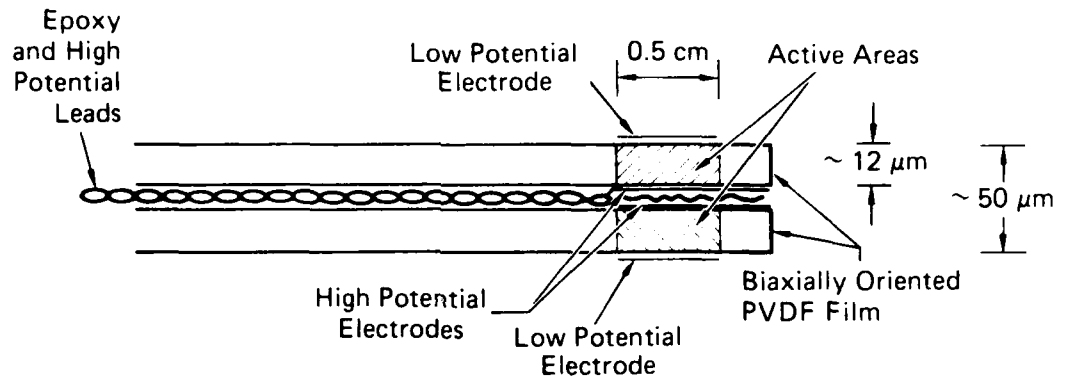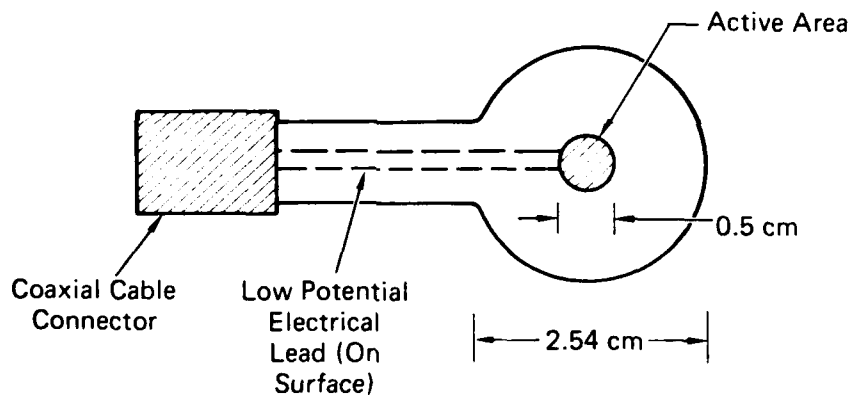
(b) Plan View

Figure 1.   PVDF sensing element of the NBS polymer soil stress gage.

5

SECTION 3

EXPERIMENT DESIGN

The combined loading by longitudinal and shear waves was produced using SRI's inclined-impact gas gun facility.[8] This gas gun produces plane parallel impact of the flyer plate and target with both equally inclined to the direction of motion of the flyer plate (Figure 2). Upon impact both a longitudinal and shear plane wave propagate into the target and the flyer plate. The normal-impact experiment was performed using the same gas gun with the flyer plate and target not inclined.

The targets in these plate-impact experiments consisted of the PVDF sensing element epoxied in place between two layers of polymethyl methacrylate (PMMA). The epoxy layers were nominally 13-μm thick, and epoxy filled the volume between the two PMMA buffers beyond the radius of the PVDF element. PMMA was also used for the flyer plates that impacted the targets. PMMA was well suited to these experiments because its shock impedance is close to that of PVDF, and the wave velocities in the material were known from an earlier study.[9] For an impact velocity of 0.270 mm/μs, the longitudinal (shock) wave travels at 3.14 mm/μs and the trailing shear wave travels at 1.54 mm/μs. These two waves separate as they propagate through the front PMMA buffer (nominally 2-mm thick in Experiments 2 through 4), with the longitudinal wave arriving at the PVDF sensing element 0.7 μs after impact and the shear wave arriving nearly 1.5 μs after impact. The delay of the arrival of the shear wave was convenient for distinguishing any potential shear sensitivity from the normal stress sensitivity of the PVDF element. The release wave from the rear of the flyer plate (nominally 7-mm thick in all experiments) arrived at the PVDF element nearly 5 μs after impact.

The shear stress transmitted through the PVDF element is deduced from measurements of the transverse particle velocity in the rear PMMA buffer. The particle veloc-ities in the interior of one or both buffer plates are measured using embedded electromagnetic gages that operate according to the electromagnetic law for moving circuits

$$\epsilon = \vec{l} \bullet (\vec{u} \times \vec{B}) \tag{5}$$

where ϵ is the electromotive force (emf) generated by a conductor moving in the constant magnetic field $\vec{B}$. The particle velocity gage, whose length and orientation are denoted by the vector $\vec{l}$, is the conductor, and it moves with the velocity of the surrounding material $\vec{u}$. The magnetic field is produced by a pair of electromagnets that surround the entire target. The relative contributions from the dipole magnet and the solenoid magnet are adjusted to align the magnetic field perpendicular to the target.[8] With this orientation, the transverse particle motion, which is along the vertical direction in the plane of the impact surface (Figure 2), will generate an emf in the particle velocity gages that extend across the width of the target (out of the page in Figure 2). Equation (5) illustrates that this emf is directly proportional to the transverse particle velocity.

For steady, one-dimensional waves, either longitudinal or shear, the stress jump across the wave front is given by the Hugoniot jump condition[8]
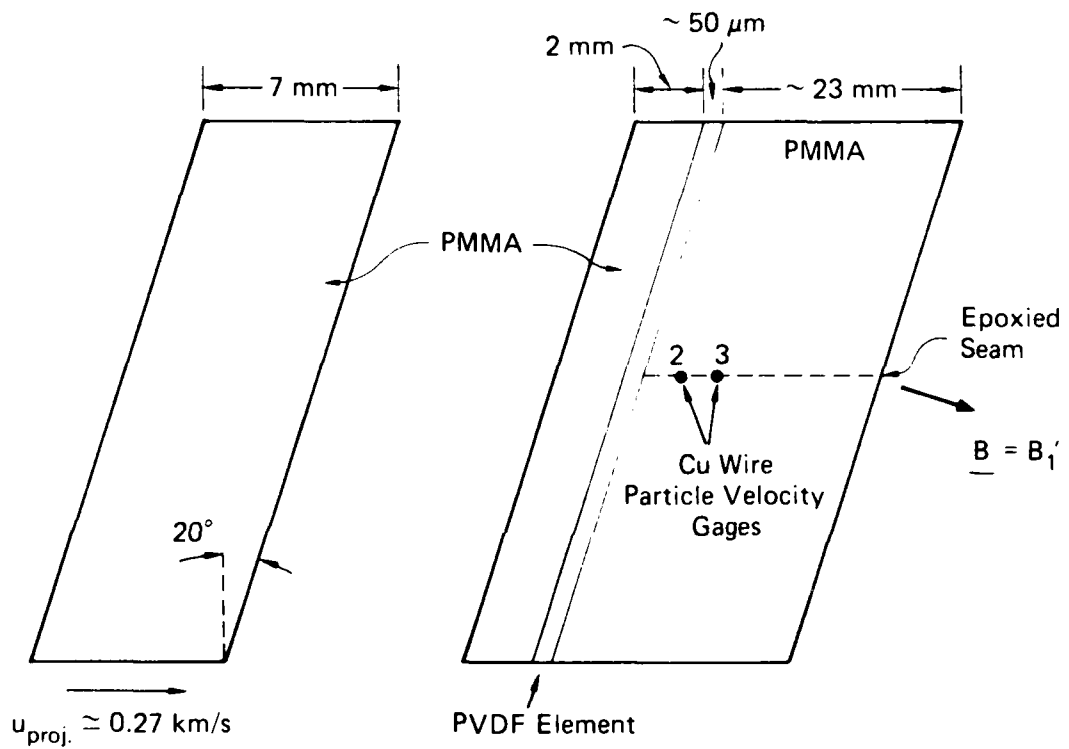
Figure 2. Configuration of inclined-impact experiments (a thin metalic film element is vapor deposited onto the impact surface of the target to serve as particle velocity gage 1).

7

$$\sigma = \rho \, U \, u \qquad \qquad (6)$$

When Equation (6) is applied to a shear wave, σ is the shear stress behind the wave front, ρ is the density of the material ahead of the shear wave compressed by earlier passage of a longitudinal wave, and U and u are the shear wave speed and the measured transverse particle speed, respectively.

We performed four experiments. The thickness of the flyer plate in all four experiments was 7 mm. In Experiments 1, 3, and 4 the flyer plate and target were inclined 20° to the direction of motion of the flyer. In Experiment 2 the target was subjected to normal-impact, producing no shear. In an effort to keep the number of experiments to a minimum, we chose to make the first experiment an inclined-impact. Because the response of PVDF to normal impact was qualitatively known from earlier work,[10] this experiment had the potential of immediately identifying the existence of a piezoelectric sensitivity to shear stress.

The target assembly used in Experiment 1 differed from that of the succeeding experiments. In this target, thin metal foils that served as particle velocity gages were embedded inside each PMMA buffer and also epoxied into the interface between the PVDF and the buffer plates. The transverse particle velocity was in the plane of the epoxy seams, which are zones of reduced strength. We attempted to measure the polarization of the PVDF through the charge accumulated on a known capacitance connected in parallel to the sensing element. The signal recorded in this experiment (see Section 4) was filled with noise and difficult to interpret. The electrical response of the PVDF should follow the stress loading history, first reacting to the longitudinal shock wave and then, approximately 0.5 µs later, reacting to the transverse wave. Although the response of the PVDF element to a longitudinal stress wave was qualitatively known from earlier work,[10] we could not distinguish whether a sensitivity to shear affected the record. The results indicated the need for modifying the design of the target and the circuit that recorded the signal produced by the PVDF sensing element.

The targets for the remaining experiments included three improvements. First, gages were omitted from the interior of the front buffer plate. A front surface particle velocity gage was placed on the front buffer. Thus there was no epoxy-bonded seam in the 2.0-mm-thick front buffer. Second, fine copper wires were used as the particle velocity gages, and these were positioned 1 and 2 mm from the PVDF gage in the 23-mm-thick rear buffer plate. The change in gage material and gage position reduced the capacitive coupling to the PVDF gage's response that was apparent in the first experiment. (Compare the shapes of particle velocity gages 2 and 3 with that of the PVDF element in Section 4.) The third improvement in the mechanical design of the target was to make the cut in the rear PMMA buffer for placing the copper wire gages perpendicular to both the direction of wave propagation and the transverse particle velocity so that the shear would be transmitted well and the motion of the particle velocity gages would closely follow that of the material.[9]

Improvements were also made in the circuit used to record the signal from the PVDF element. In Experiment 1, three types of coaxial cables totaling 21 m in length connected the PVDF element to a parallel capacitor of 105.4 nF. This capacitor was located directly across the terminals of the oscilloscope terminated in 50-Ω resistance. This circuit recorded the maximum charge difference on the

electrodes of the PVDF induced by its change in polarization. Terminating the circuit created an RC decay time of 5 μs, causing the capacitor to lose its charge too quickly. The high frequency noise in the record may result from impedance mismatch existing in the circuit. The lower frequency noise superposed on the exponentially decaying voltage on the capacitor may arise from the interaction of the capacitor and line resistance with the 55-μH distributed line inductance.

In all succeeding experiments, we recorded the current flowing between the electrodes of the PVDF element rather than the charge difference created by polarization. The PVDF element was connected in series by total of 4.5 m of coaxial cables to a large (5-kΩ or 50-kΩ) resistance. The voltage drop across 50 Ω of this resistance was monitored by an oscilloscope terminated in 50-Ω resistance. This voltage-divider configuration was adopted to provide a better impedance match along the circuit. The length of cable was reduced to minimize effects of line inductance.

The response of this circuit was tested in a normal-impact experiment, Experiment 2, for which the current response of the PVDF element was known. As discussed below, the results from Experiment 2 satisfactorily demonstrated that the measuring circuit was transmitting the response of the PVDF gage without excessive perturbation. Since this experiment was performed, however, several deficiencies in this circuit have been brought to my attention.[11] The major deficiency of this revised circuit design is that it did not provide complete impedance matching at the high frequencies that were of interest.

SECTION 4

RESULTS

As described in Section 3, deficiencies in the design of Experiment 1 made the results uninformative. The modifications to the mechanical design of the target and the recording circuit were tested in the normal-impact experiment, Experiment 2. Following the favorable result of Experiment 2, we expected to be able to conclude this study with two additional inclined-impact experiments. In Experiment 3 we recorded the response of the PVDF element and measured the transverse particle velocities. To remove the potential influence of the magnetic field on the response of the PVDF element recorded in Experiment 3, Experiment 4 replicated that experiment with no magnetic field present. As discussed in detail in Section 5, the results from these two experiments are inconclusive. Within the term of this project, we could not obtain additional specimens for further experiments to determine the cause of the unexpected response of the PVDF element.

In section 5 we discuss differences in the construction of the targets that could have caused the disturbance of the response of the PVDF elements. In the following paragraphs we present the results of the individual experiments and the details their construction and execution.

EXPERIMENT 1 (85-2-21)

The construction of the target and the measuring circuit in this experiment are described above. The front and rear PMMA buffers were 3.0-mm and 8.1-mm thick, respectively. The PVDF element was NBS gage N-20, having a static capacitance of 1.43 nF. The exterior electrodes on this element covered its entire area (see Figure 1). The effective hydrostatic d-constant of this specimen, determined by Bur using a drop-test technique,[1] was 25.6 pC/N. The inclined flyer plate impacted the inclined target at a velocity of 0.29 km/s. The target was positioned in a uniform magnetic field of 1503 Gauss, directed along the vertical, perpendicular to the direction of motion of the flyer plate. With the magnetic field in this orientation, the particle velocity gages were sensitive to longitudinal and transverse motion in the ratio of $1:\sin 20°$.

Figure 3 shows the digital recording of the response of the PVDF element connected in parallel to a 105.4-nF capacitor. This record was produced by a Nicolet 2093 oscilloscope with a 205A plug-in unit sampling the signal at 20-ns intervals. The voltage output was converted to charge by multiplying by 106.83 nC, the effective capacitance of the circuit elements. Figure 4 shows analog recordings of the response of the PVDF element and particle velocity histories at the particle velocity gage in the front buffer plate (Gage 1) and the ones adjacent to each face of the PVDF element (Gages 2 and 3). These records were recorded on Tektronix 7704A oscilloscopes. The arrival of the transverse wave at Gage 1, 0.5 mm from the impact surface, can be seen as the inflection near the first peak in the record from that gage. The horizontal scale in each photo is 0.5 μs per division. The vertical scales are 1 V per division for the PVDF record, and 0.05 V per division for the particle velocity gages.

EXPERIMENT 2 (85-2-25)

The purpose of this experiment was to test modifications in the design of the experiment. The target for this experiment followed the modified design described above, except it contained no particle
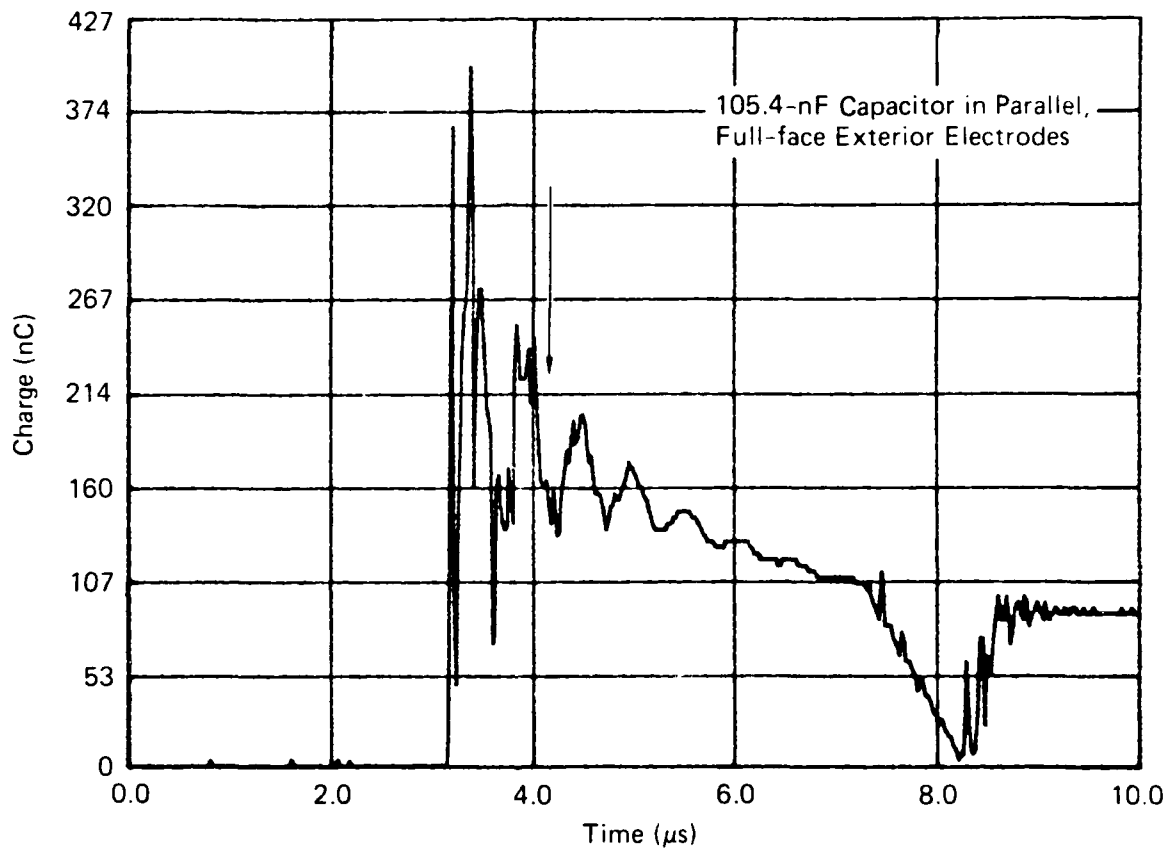
Figure 3.   Digital recording (20 ns/point) of response of PVDF element
in Experiment 1 (85-2-21) (the arrow marks the arrival time
expected for the transverse wave).

11
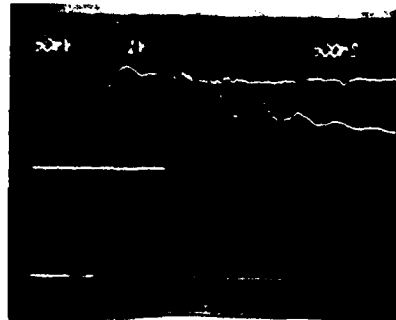
(a) Particle Velocity Gage 1 (Upper) and PVDF Element (Lower).
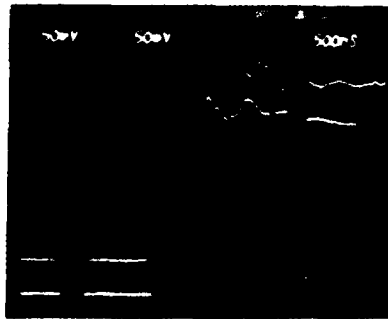
(b) Particle Velocity Gages 2 (Upper) and 3 (Lower).

Figure 4. Experiment 1 (85-2-21) records.

velocity gages. The PVDF element was NBS gage N-4, having a static capacitance of 1.29 nF. The exterior electrodes of the PVDF element covered only the central 0.5-cm-diameter sensitized region. The effective hydrostatic d-constant of this specimen was 42.0 pC/N. No magnetic field was applied, and the velocity of the normal impact was 0.267 km/s.

Figure 5 shows the digital recording of the response of the PVDF element connected in series to a 50-kΩ resistor. The signal was sampled at 20-ns intervals. The voltage output was converted to current by dividing by 50 Ω, the resistance across the terminals of the oscilloscope. This record quali-tatively is very similar to the observations of Bauer[10] in similar normal-impact experiments. The tilt of the impact in this experiment was less than 0.1°. Figure 6 shows the history of the charge difference on the electrodes of the PVDF element obtained by integrating the current-time history of Figure 5.

EXPERIMENT 3 (85-2-26)

In this inclined-impact experiment, we measured the response of the PVDF sensing element pack-aged in a target having the modified design described in the previous section. We also measured the transverse particle velocity in each of the buffer plates to calculate the shear stress transmitted through the PVDF from Eq. (6). The PVDF element was NBS gage N-19, having a static capacitance of 1.44 nF. The exterior electrodes of the PVDF element covered its entire surface. The effective hydrostatic d-constant of this specimen was 31.3 pC/N. The impact velocity was 0.270 km/s.

The target was positioned in a uniform magnetic field of 2275 Gauss, oriented along the normal to the impact surface. This orientation rendered the particle velocity gages sensitive only to transverse particle motion (along the vertical direction in the plane of the impact surface). Due to the limited precision with which the orientation of the magnetic field can be set, contributions from the much larger longitudinal particle motion can be identified in records from Gages 2 and 3.

Figure 7 shows these records along with the response of the PVDF element. The PVDF element was connected in series to a 5-kΩ rather than a 50-kΩ resistor. The series resistance was reduced to increase the signal amplitude. We do not believe this change caused any significant reduction in response time of the circuit. The horizontal scales in both photos in Figure 7 are 1 μs per division. The vertical scale in Figure 7(a) is 0.04 A per division for the PVDF record and 18.20 m/s per division for Gage 3. The vertical scale in Figure 7(b) is 10.08 m/s per division for Gage 2 and 12.74 m/s per division for Gage 3. Figure 8 shows digital recordings of the particle velocity histories at the front sur-face (Gage 1) and 2 mm behind the PVDF element (Gage No. 3). The Nicolet oscilloscopes sampled these signals at 50-ns intervals.

EXPERIMENT 4 (85-2-27)

This inclined-impact experiment replicated Experiment 3 except that no magnetic field was applied. The particle velocity gages were present, but not connected in a closed electrical circuit. The PVDF element was NBS gage N-21, having a static capacitance of 1.21 nF. The exterior electrodes of the PVDF element covered its entire surface. The effective hydrostatic d-constant of this specimen was 29.2 pC/N. The impact velocity was 0.274 km/s. Figure 9 shows digital and analog records of

13
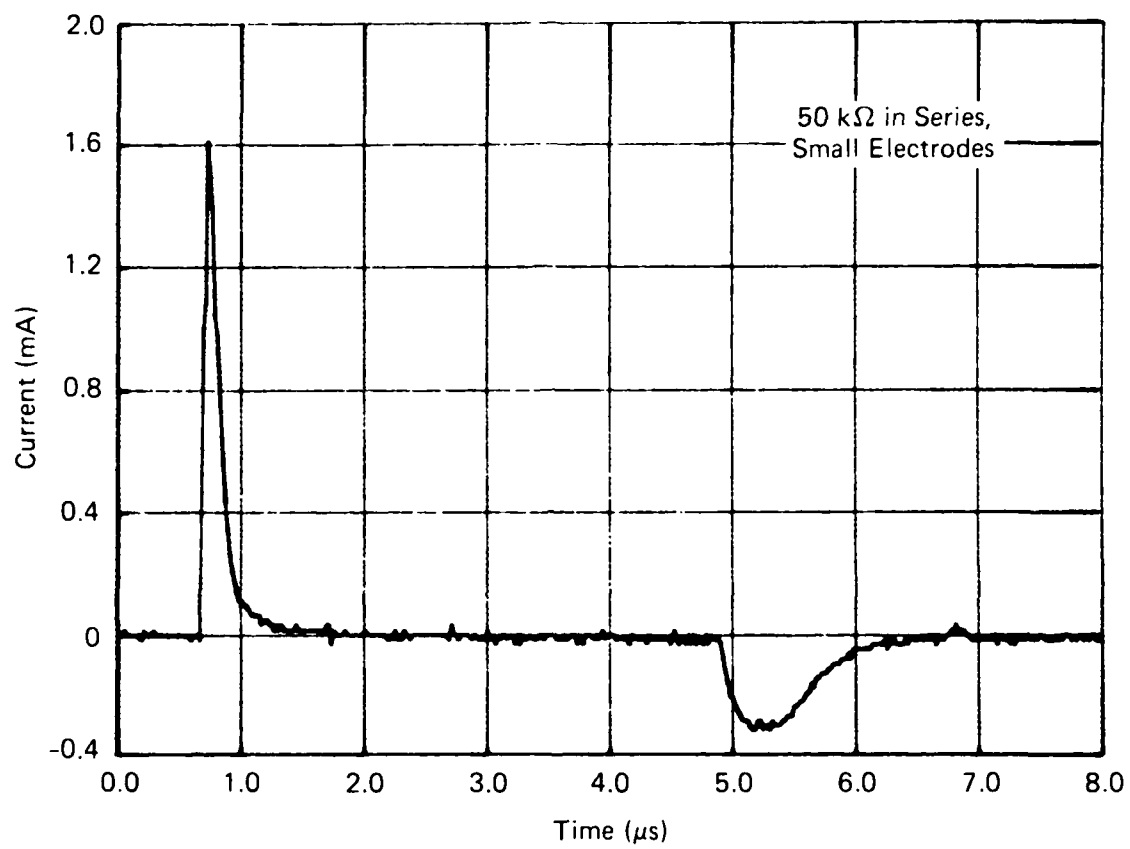
Figure 5.   Digital recording (20 ns/point) of response of PVDF element
in Experiment 2 (85-2-25).
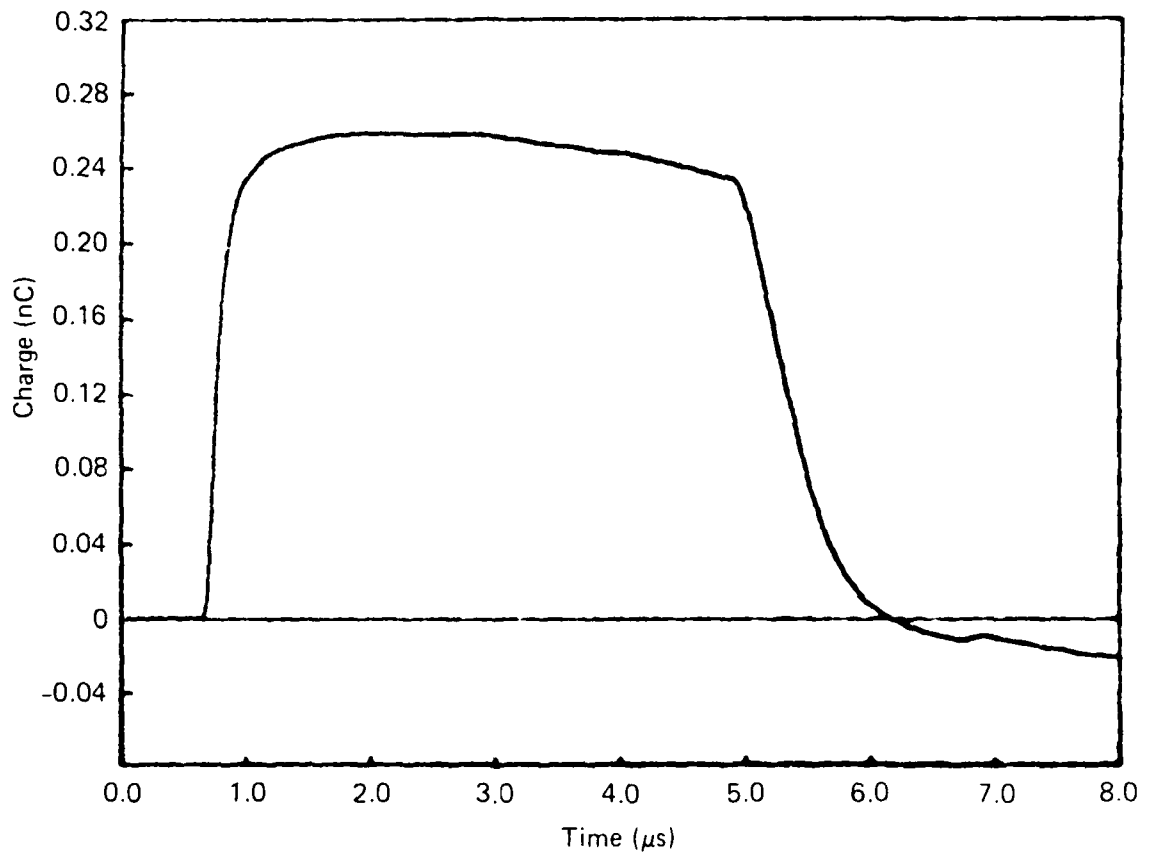
Figure 6.   Charge difference on electrodes of PVDF element
obtained by integrating current history in Figure 5.
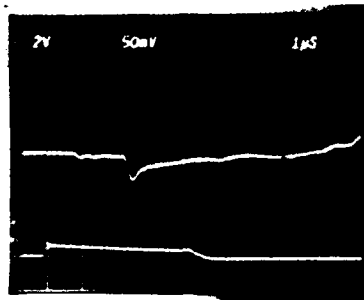
1.0 μs/cm

(a) Particle Velocity Gage 3 (Upper)
and PVDF Element (Lower).
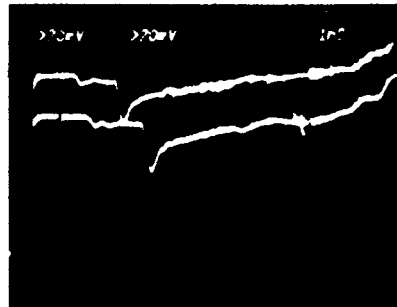
1.0 μs/cm

(b) Particle Velocity Gages 2 (Upper)
and 3 (Lower).

Figure 7. Experiment 3 (85-2-26) records.
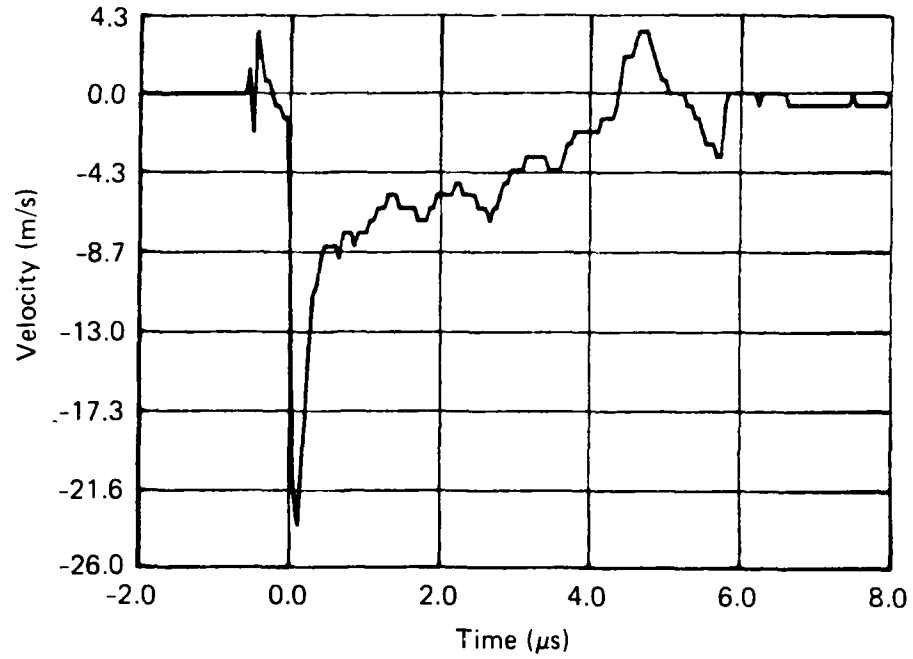
(a) Particle Velocity Gage 1
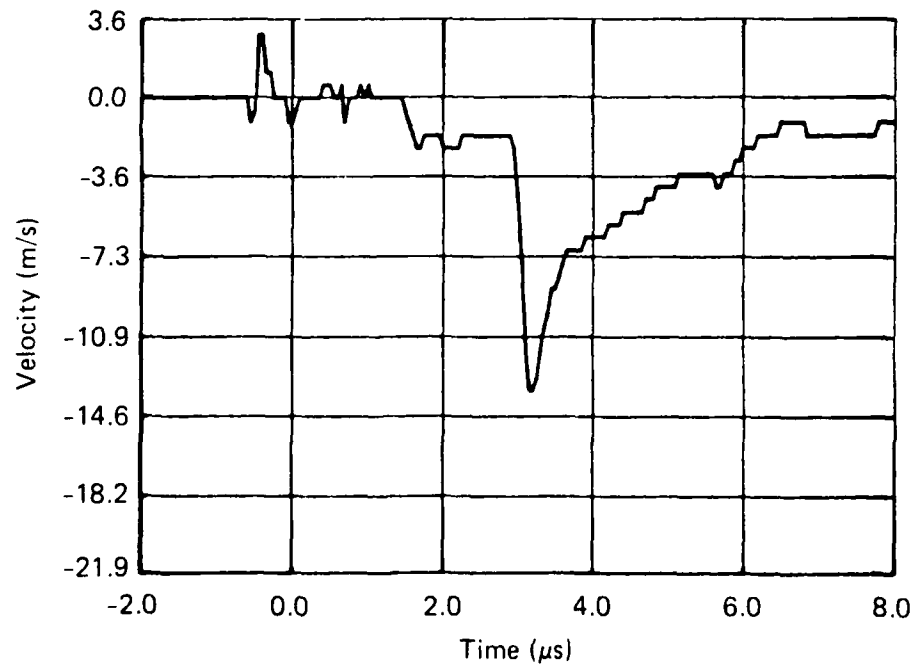
(b) Particle Velocity Gage 3

Figure 8. Digital (50 ns/point) particle velocity records
from Experiment 3 (85-2-26).
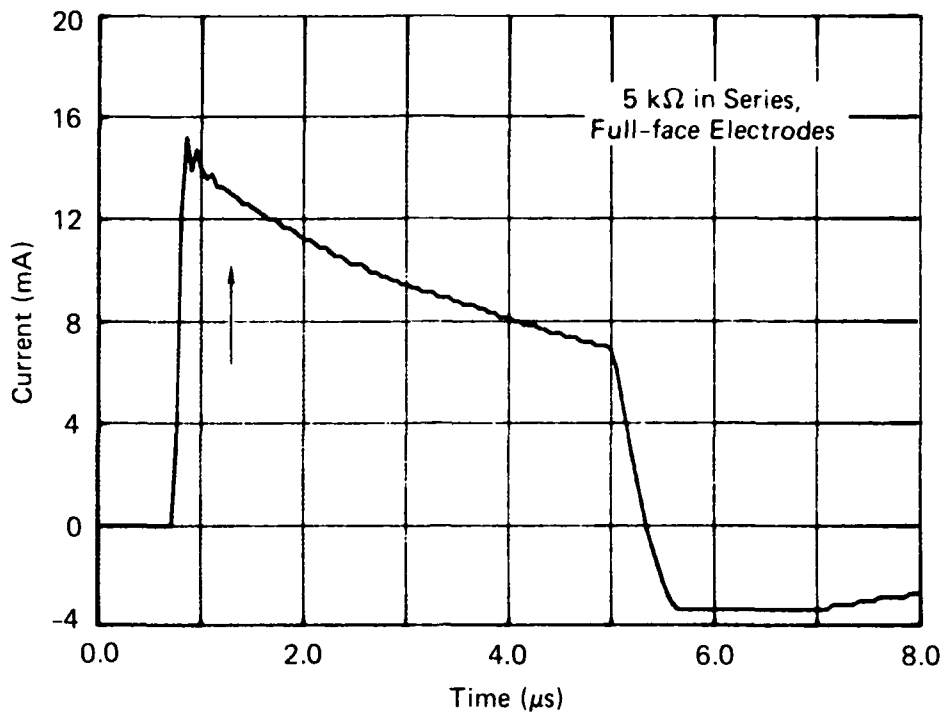
(a) Digital Recording (50 ns/point)
(The arrow marks the arrival time
expected for the transverse wave).
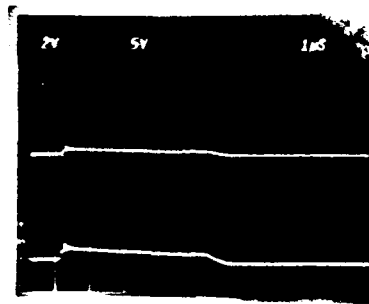
(b) Analogue Recording at Two
Different Amplifications

Figure 9. Response of PVDF element recorded in Experiment 4
(85-2-27).

the response of the PVDF element. The digital signal in Figure 9(a) was obtained by sampling the signal at 50-ns intervals. The voltage output was converted to current by dividing by 50 Ω, the resistance across the terminals of the oscilloscope. The horizontal scales in Figure 9(b) are 1 μs per division, and the horizontal scales are 0.10 A per division for the upper trace and 0.04 A per division for the lower trace.

SECTION 5

ANALYSIS AND DISCUSSION

We first discuss the results of the normal-impact experiment (Experiment 2) to provide the baseline for comparison with the results of the incline-impact experiments. As mentioned above, the response of the PVDF element shown in Figure 5 is comparable to that seen in earlier work by Bauer.[10] As with quartz gages,[12] a current is generated by the piezoelectric material as long as there is a difference in the stress on its faces. Thus the current signal lasts for the time it takes a stress change to cross the specimen. Because the PVDF specimen is very thin, the current pulse is a spike. Impact tilt and the response time of the electrical circuit contribute to the width of the spike in Figure 5. The broader current pulse with the opposite sense around 5 μs is the signal produced as the broader front of the release wave propagates through the PVDF.

Quantitative analysis of the record from Experiment 2 reveals a deficiency in the experiment. We use the charge generated by the stress wave to calculate an effective d-constant relating stress to polarization. The change in charge measured in the experiment is related to the change in polarization by

$$\frac{dQ}{d\sigma} = A\frac{dP}{d\sigma} + P\frac{dA}{d\sigma} \tag{7}$$

where Q is charge, P is polarization, and A is the sensitized area. Under the uniaxial strain conditions in this experiment, A does not vary (dA = 0), and all three normal components of the stress σ are compressive. For an order-of-magnitude estimate, we ignore the contributions of the two normal stresses in the plane of the PVDF element and take 0.25 nC as a nominal value for dQ (Figure 6). The magnitude of the through-the-thickness normal stress was approximately 4.5 kbar (450 MPa).[9] Using these values in Eq. (7) we obtain

$$d_{33} = \frac{1}{A}\frac{dQ}{d\sigma} = \frac{0.25 \text{ nC}}{0.785 \text{ cm}^2 \text{ x } 45,000 \text{ N/cm}^2} = 0.0071 \text{ pC/N} \tag{8}$$

Here the subscript on the d-constant refers to the film coordinate system. If the effective constants d_{31} and d_{32} are positive, Eq. (8) provides an upper bound on the effective constant d_{33}. Assuming d_{33} is of the same order of magnitude as d_{31} and d_{32}, it should be comparable to the effective hydrostatic d-constant of 42 pC/N determined by Bur.[1] The cause of this inconsistency in unknown. Using Equation (2) to account for the effect of the adiabatic temperature rise in the experiment would increase the disagreement.

In the inclined-impact experiments, a transverse wave follows the longitudinal shock wave at a slower speed. The thickness of the flyer plate is chosen so that this transverse wave front reaches the PVDF before the faster-traveling relief wave. Thus we expect any piezoelectric sensitivity that PVDF may have to shear stress to be manifest as a current pulse occurring in the record in the quiescent

20

interval between the two pu..ses seen in Figure 5. Because the transverse wave is a simple wave like the relief wave rather than a shock wave, we expect any current pulse produced by it to be broad. The sense of a shear-stress-induced current pulse cannot be predicted.

In Experiment 1 we recorded the charge difference between the two faces of the PVDF element rather than the current that equilibrates the charge. This is analogous to directly recording the charge history, Figure 6. From the above discussion, we expect a shear-stress sensitivity to be manifest in a charge history plot as a step, either up or down, superimposed on a plateau such as that seen in Figure 6. The charge history from Experiment 1 (Figure 3) does not have this general form, and no contribution to the signal from the transverse wave can be identified. The dip seen around 8 μs is produced by the relief wave. We do not know the reason for the discrepancy.

In Experiments 3 and 4 we measured current histories, as in Experiment 2. The response of the PVDF element is unaffected by the presence of a magnetic field, as seen by comparing Figure 7(a) with Figure 9(b). In both figures, the shape of the current history is very different from that seen in Figure 5 for the normal-impact experiment. These records are peculiar because the pulses expected from the results of Experiment 2 are absent, and they deviate from the shape of the record from Experiment 2 even before the transverse wave arrives at the PVDF element. Indeed, these current history records from Experiments 3 and 4 more closely resemble the charge history record of Experiment 1.

We have been unable to determine the reason for these peculiarities. The exterior electrodes of the PVDF element in Experiment 2 covered only the central 0.5-cm-diameter sensitized region. In the other experiments, these electrodes covered the entire area of the element. Additionally, the target in Experiment 2 contained no particle velocity gages. Beyond these differences is only the difference in impact orientation; Experiment 2 was a normal impact, while the other experiments were all inclined impacts. Variations in the measuring circuit among the experiments do not correlate with peculiarities in the PVDF signal records.

The particle velocity records from Experiment 3 allow us to estimate the magnitude of the shear stress transmitted through the PVDF element. We consider Gage 3 first. In Figure 8(b) the steep jump from approximately 2 m/s to 13.5 m/s about 3 μs after impact is the contribution from the transverse particle motion. Using the original digital voltage-time record, we calculate 11.5 $\pm$ 0.4 m/s for the transverse particle speed at Gage 3. We obtain 11.2 m/s and 11.3 m/s from the two analog oscilloscope recordings of Gage 3 shown in Figure 7. For Gage 2, from two analog oscilloscope recordings (one shown in Figure 7b), we obtain 10.4 m/s and 11.8 m/s for the transverse particle speed. These values are consistent with the propagation of a steady transverse wave in the rear PMMA buffer.

To calculate the transverse particle speed at the front surface of the target, we subtract the contribution from the longitudinal particle motion, which arises from imperfect alignment of the magnetic field, from the peak value of approximately 23.5 m/s in Figure 8(a). We assume that the contribution from the longitudinal particle motion is the same as at Gage 3. Using the original digital voltage-time record, we calculate 21.5 $\pm$ 0.5 m/s for the transverse particle speed at Gage 1.

Using these speeds in Equation (6), we obtain estimates of the applied and transmitted shear stress. Following Gupta,[9] we take 1.185 g/cm^3 and 1.043, respectively, for the initial density and compression of PMMA in this experiment, and 1.54 km/s for the transverse wave speed. At Gage 1 we obtain an applied shear stress of 0.41 ± 0.01 kbar (41 MPa), and at Gage 3 we obtain a shear stress of 0.22 ± 0.01 kbar (22 MPa). Note that the value for shear stress at the front surface is overestimated if the transverse wave was not steady when it was generated. For comparison, the shear stress calculated using the COPS program[13] to simulate this experiment is 0.77 kbar (77 MPa) when purely elastic response is assumed and no slipping is allowed at the PMMA-PVDF interfaces.

SECTION 6

CONCLUSIONS AND RECOMMENDATIONS

In the records from the inclined-impact experiments, we observe no variation that would correspond to the arrival of the transverse waves. If we assume that the causes of the peculiarities in these records did not suppress the effects of the transverse waves, we can estimate an upper bound on the relative piezoelectric sensitivity of PVDF to in-plane shear stress from the measured shear stress. For this estimate, we assume that the normal stresses existing in the uniaxial strain state are equivalent to a hydrostatic stress. We treat the peak current value in a PVDF record as arising from a hydrostatic stress of 4.5 kbar (450 MPa).

Figure 9(a) shows a resolution of 0.2 mA, the best obtained in a PVDF record. This is 1/75 of the peak value and, by assumption, is greater than the contribution from the 0.22-kbar (22 MPa) shear stress. The ratio of the peak current produced by the approximately hydrostatic stress to the peak current produced by the in-plane shear stress equals the ratio of the contributions of each stress to the polarization. This ratio is greater than 75. Dividing by 20.5, the ratio of the approximately hydrostatic 4.5-kbar stress to the 0.22-kbar shear stress, provides an estimate of the upper bound on the ratio of the effective hydrostatic d-constant to the effective shear stress d-constant.

Thus, we conclude that the piezoelectric sensitivity of PVDF to in-plane shear stress is less than 0.27 (20.5/75) times its sensitivity to hydrostatic stress. However, due to the many uncertainties in the results of our experiments, this conclusion must be regarded as tentative. Moreover, the polarization-stress relation for PVDF is likely to be nonlinear because of its large compliance and because much of its response is likely to be secondary piezoelectricity. In applying the present bound on PVDF's sensitivity to in-plane shear to other loading conditions, corrections are needed to account for these nonlinearities.

It is clear that PVDF is potentially very useful as a stress transducer.[1-3] However, many questions about its piezoelectric response to large magnitude dynamic stress need to be answered even before a gage package is designed. Future work on PVDF should be conducted on specimens that can be replicated with high precision. These specimens should be a simple configuration of one layer of PVDF. It may be useful to include a guard ring[14] with the electrodes applied to the PVDF. Further consideration must be given to choosing an electrical circuit for measuring the response of the PVDF element. The extreme thinness of the film and the resolution desired in the measurements should be accommodated by the chosen circuit. In inclined-impact experiments, where the peak longitudinal stress is always substantially larger than the peak shear stress, the resolution of the measurements determines the minimum detectable sensitivity to shear stress.

The SRI split Hopkinson torsion bar [15] (SHTB) could be an alternative to inclined-impact experiments that would reduce the need for high-resolution measurements. With this method, approximately uniform millisecond-duration shear stress can be applied over an annular region with or without application of a static through-the-thickness compression. Torsion bar experiments would have the advantages of allowing the ratio of shear to normal stress to be varied over a greater range and of potentially requiring less effort.

23

In a recent review, Broadhurst and Davis[16] discuss many of the proposed mechanisms of secondary piezoelectricity that could contribute to the sensitivity of PVDF. Due to the complexity, it is unlikely that the piezoelectric response of PVDF can be modeled accurately as a collection of physical mechanisms. Instead, it will have to be described on a phenomenological basis, much as the piezoelectric behavior of quartz[12] and lithium niobate[17] are. The physical mechanisms Broadhurst and Davis discuss all depend differently on stress, strain, and temperature. Any one mechanism will be linear in any of these three variables over a limited range only. The composite effect of two or more mechanisms may be completely nonlinear in these variables. The ranges for stress, strain, and temperature for which the piezoelectric response of PVDF is linear need to be identified. Nonlinear response will require that a gage package containing PVDF be calibrated under conditions very similar to those in which it will be fielded. In particular, if the piezoelectric response of PVDF to longitudinal stress is nonlinear in the stress range of interest, then it is inappropriate to assume that its response to combined loading by a longitudinal wave followed by a shear wave is equivalent to the superposition of its response to each wave separately.

Both the inclined-impact and the SHTB techniques will be useful for investigating the variation of the piezoelectric response of PVDF over the range of stress and strain of interest for field applications. Additional useful fundamental measurements of the behavior of PVDF could be conducted under quasi-static, unstressed conditions using the piezoelectric resonance method.[18] Auld and Gagnepain[19] used this technique to investigate the temperature dependence of the piezoelectric (in-plane) shear coupling constant from 0°C down to liquid-helium temperature. They were able to obtain only qualitative estimates of effective piezoelectric stress constants e_{15} and e_{24}. Further work would be needed to determine if this method could provide quantitative estimates of these effective piezoelectric constants.

Auld and Gagnepain assumed that the macroscopic symmetry of the uniaxially stretched film they studied was mm2. As mentioned above, we have not found a conclusive determination of the symmetry of the bulk film. The resonance technique is flexible enough to allow many of the effective piezoelectric constants to be measured. Thus, relatively extensive measurements could be made with no confining stress, and possibly with confining stress as well. These measurements might be an efficient means of investigating the symmetry properities of the film, which is an important step toward describing its general piezoelectric response.

SECTION 7

LIST OF REFERENCES

1. A. J. Bur and S. C. Roth, "Measurement of a Piezoelectric d Constant for Poly (vinylidene fluoride) Transducers Using Pressure Pulses," J. Appl. Phys. 57 , 113 (1985).

2. A. J. Bur and S. C. Roth, " A Polymer Pressure Gage For Dynamic Pressure Measurements," in Proceedings of the Second Symposium on the Interaction of Non-nuclear Munitions with Structures, April 15-18, 1985, p. 291.

3. R. M. Chung, A. J. Bur, and J. R. Holder, "Laboratory Evaluation of an NBS Polymer Soil Stress Gage," p. 296 in reference 2.

4. J. R. Holder, R. M. Chung, and A. J. Bur, "Field Evaluation of the Polymer Soil Stress Gage," p. 302 in reference 2.

5. R. G. Kepler and R. A. Anderson, "Piezoelectricity in Polymers," CRC Critical Reviews in Solid State and Materials Sciences 9 , 399 (1980).

6. M. G. Broadhurst, G. T. Davis, J. E. McKinney, and R. E. Collins, "Piezoelectricity and Pyroelectricity in Polyvinylidene Fluoride--A Model," J. Appl. Phys. 49 , 4992 (1978).

7. A. S. DeReggi, S. Edelman, and S. C. Roth, "Piezoelectric Polymer Transducers for Dynamic Pressure Measurements," National Bureau of Standards Internal Report, NBSIR 76-1078 (June 1976).

8. Y. M. Gupta, "Development of a Method for Determining Dynamic Shear Properties," Draft Final Report submitted to the Defense Nuclear Agency under Contract DNA001-76-C-0384, SRI International, Menlo Park, California, May 1978 (unpublished).

9. Y. M. Gupta, "Determination of the Impact Response of PMMA Using Combined Compression and Shear Loading," J. Appl. Phys. 51 , 5352 (1980).

10. F. Bauer, "PVF$_2$ Polymers: Ferroelectric Polarization and Piezoelectric Properties Under Dynamic Pressure and Shock Wave Action," Ferroelectrics, 49 , 231 (1983).

11. Drs. D. Tasker and F. Bauer, personal communication.

12. R. A. Graham, "Strain Dependence of Logitudinal Piezoelectric, Elastic, and Dielectric Constants of X-cut Quartz," Phys. Rev. B, 6 , 4779 (1972).

13. Y. M. Gupta, "Calculation of P and S Waves (COPS): Wave Propagation Program," (unpublished).

14. R. A. Graham, F. W. Neilson, and W. B. Benedick, "Piezoelectric Current from Shock-loaded Quartz--A Submicrosecond Stress Gauge," J. Appl. Phys. 36 , 1775 (1965).

15. D. A. Shockey, D. R. Curran, and L. Seaman, "Development of Improved Dynamic Failure Models," Section III in Final Technical Report by SRI International, submitted to U. S. Army Research Office under Contract DAAG-29-81-K-0123 (February 1985).

16. M. G. Broadhurst and G. T. Davis, "Physical Basis for Piezoelectricity in PVDF," Ferroelectrics 60, 3 (1984).

17. Y. M. Gupta, "Theoretical and Experimental Studies to Develop a Piezoelectric Shear Stress Interface Gage," Draft Final Report DNA-84-342 Revised, submitted to Defense Nuclear Agency under Contracts DNA001-80-C-0145 and DNA001-82-C-0297 (August 1984).

18. H. Ohigashi, "Electromechanical Properties of Polarized Polyvinylidene Fluoride Films as Studied by the Piezoelectric Resonance Method," J. Appl. Phys. 47, 949 (1976).

19. B. A. Auld and J. Gagnepain, "Shear Properties of Polarized PVF_2 Film Studied by Piezoelectric Resonance Method," J. Appl. Phys. 50, 5511 (1979).

DISTRIBUTION LIST

DEPARTMENT OF DEFENSE

DEFENSE ADVANCED RSCH PROJ AGENCY
    ATTN: DIRECTOR

DEFENSE INTELLIGENCE AGENCY
    ATTN: RTS-2B

DEFENSE NUCLEAR AGENCY
    ATTN: RAEV
    ATTN: SPAS
    ATTN: SPSS
12 CYS ATTN: SPTD
    ATTN: STNA
    ATTN: STRA
    ATTN: STSP
4 CYS ATTN: STTI-CA

DEFENSE TECHNICAL INFORMATION CENTER
12 CYS ATTN: DD

DEPT OF DEFENSE EXPLO SAFETY BOARD
    ATTN: CHAIRMAN

FIELD COMMAND DNA DET 2
LAWRENCE LIVERMORE NATIONAL LAB
    ATTN: FC-1

FIELD COMMAND DEFENSE NUCLEAR AGENCY
    ATTN: FCT
    ATTN: FCTEI
    ATTN: FCTT

FIELD COMMAND TEST DIRECTORATE
    ATTN: FCTC

NATIONAL SECURITY AGENCY
    ATTN: DIRECTOR

UNDER SECY OF DEF FOR RSCH & ENGRG
    ATTN: STRAT & SPACE SYS (OS)

DEPARTMENT OF THE ARMY

HARRY DIAMOND LABORATORIES
    ATTN: C KENYON
    ATTN: HD-NW-P J MESZAROS 20240
    ATTN: M BUSHELL
    ATTN: R GRAY
    ATTN: SLCHD-NW-R J BLACKBURN 22000
    ATTN: SLCHD-NW-R J VANDERWALL 22800
    ATTN: SLCHD-NW-RH G MERKEL
    ATTN: SLCHD-NW-RH R GILBERT 22800

U S ARMY ATMOSPHERIC SCIENCES LAB
    ATTN: SLCAS-D CMDR/DIR

U S ARMY BALLISTIC RESEARCH LAB
    ATTN: SLCBR-TB-E P HOWE

U S ARMY COLD REGION RES ENGR LAB
    ATTN: TECHNICAL DIRECTOR

U S ARMY COMMUNICATIONS R&D COMMAND
    ATTN: COMMANDER

U S ARMY ELECTRONICS R & D COMMAND
    ATTN: DELET-ER
    ATTN: DRSL

U S ARMY ENGINEER DIV HUNTSVILLE
    ATTN: COMMANDER

U S ARMY ENGR WATERWAYS EXPER STATION
    ATTN: G P BONNER WESJV-Z
    ATTN: J INGRAM WESSER
    ATTN: R WELCH WESSE-R
    ATTN: R WHALIN WESZT
    ATTN: WESSE

U S ARMY STRATEGIC DEFENSE CMD
    ATTN: DASD-PP

U S ARMY STRATEGIC DEFENSE CMD
    ATTN: BMDSC-HW R DEKALB
    ATTN: DASD-H-SAV R C WEBB

U S ARMY STRATEGIC DEFENSE COMMAND
    ATTN: ATC
    ATTN: ATC-O F HOKE

USA ELECT WARFARE/SEC SURV & TARGET ACQ CTR
    ATTN: AMSEL-EW-SS S KRONENBERG

DEPARTMENT OF THE NAVY

DAVID TAYLOR NAVAL SHIP R & D CTR
    ATTN: CODE 1
    ATTN: CODE 174

NAVAL SURFACE WEAPONS CENTER
    ATTN: J FORBES
    ATTN: R TUSSING

NAVAL WEAPONS CENTER
    ATTN: G GREENE

27

DEPARTMENT OF THE NAVY (CONTINUED)

NAVAL WEAPONS EVALUATION FACILITY
ATTN: CLASSIFIED LIBRARY

OFFICE OF NAVAL TECHNOLOGY
ATTN: CODE 217

DEPARTMENT OF THE AIR FORCE

AIR FORCE ARMAMENT LABORATORY
ATTN: M ZIMMER

AIR FORCE OFFICE OF SCIENTIFIC RSCH
ATTN: AFOSR/NA

AIR FORCE WEAPONS LABORATORY, AFSC
ATTN: NTCO C AEBY
ATTN: NTED D COLE
ATTN: NTED E SEUSY
ATTN: NTED J RENICK
ATTN: NTEO

BALLISTIC MISSILE OFFICE/DAA
ATTN: ENSN

DEPARTMENT OF ENERGY

DEPARTMENT OF ENERGY
ATTN: DIRECTOR, OSPA

EG&G ENERGY MEASUREMENTS
ATTN: W R KITCHEN

EG&G IDAHO INC
ATTN: J EPSTEIN

UNIVERSITY OF CALIFORNIA
LAWRENCE LIVERMORE NATIONAL LAB
ATTN: B BOWMAN
ATTN: E LEE
ATTN: G E VOGTLIN
ATTN: L-10 W E FARLEY
ATTN: W A BOOKLESS

LOS ALAMOS NATIONAL LABORATORY
ATTN: C S YOUNG P-14
ATTN: D EILERS
ATTN: DIRECTOR
ATTN: G BARRASCH
ATTN: G M SMITH
ATTN: J OGLE P-14
ATTN: J TOEVS P-14
ATTN: M PONGRATZ
ATTN: M WILKE
ATTN: S STONE P-14
ATTN: T MCKOWN

OAK RIDGE NATIONAL LABORATORY
ATTN: D BARTINE
ATTN: DIRECTOR
ATTN: R L ANDERSON

SANDIA NATIONAL LABORATORIES
ATTN: DIV 7111 B VORTMAN
ATTN: ORG 7116 C W COOK
ATTN: ORG 7116 S R DOLCE
ATTN: 7112 C W SMITH

OTHER GOVERNMENT

DEPARTMENT OF COMMERCE
ATTN: SEC OFC FOR INSTR DIV
ATTN: SEC OFC FOR O PETERSONS
ATTN: SEC OFC FOR OFFICE OF DIRECTOR
ATTN: SEC OFC FOR R H MCKNIGHT

FEDERAL EMERGENCY MANAGEMENT AGENCY
ATTN: OFC OF RSCH/NP H TOVEY

NATIONAL BUREAU OF STANDARDS
ATTN: A BURR
ATTN: M BROADHURST
ATTN: R E LAWTON

DEPARTMENT OF DEFENSE CONTRACTORS

ACUREX CORP
ATTN: PRESIDENT W DEAN

ADVANCED RESEARCH & APPLICATIONS CORP
ATTN: J STANLEY
ATTN: M BOYLE
ATTN: R ARMISTEAD

APPLIED RESEARCH ASSOCIATES, INC
ATTN: N HIGGINS

APTEK, INC
ATTN: T MEAGHER

ASTRON RESEARCH & ENGINEERING
ATTN: J HUNTINGTON

BDM CORP
ATTN: B BENDOW

CALIFORNIA RESEARCH & TECHNOLOGY, INC
ATTN: K KREYENHAGEN
ATTN: M ROSENBLATT
ATTN: S SCHUSTER

CALIFORNIA RESEARCH & TECHNOLOGY, INC
ATTN: F SAUER

CALSPAN CORP
ATTN: PRESIDENT

CARPENTER RESEARCH CORP
ATTN: H J CARPENTER

CHARLES STARK DRAPER LAB, INC
ATTN: P KELLY

DEPT OF DEFENSE CONTRACTORS (CONTINUED)

CUSHING ASSOCIATES, INC
    ATTN: V CUSHING

DEVELCO, INC
    ATTN: PRESIDENT

ECTRON CORP
    ATTN: E CUNNINGHAM

EG&G WASH ANALYTICAL SVCS CTR, INC
    ATTN: A BONHAM
    ATTN: G SOWER
    ATTN: M GRUCHALLA

EG&G/KIRTLAND
    ATTN: S ORRELL

EG&G, INC
    ATTN: E C SHIVERS
    ATTN: L F SANDOVAL
    ATTN: N F COCHRANE
    ATTN: P A ZAGARINO
    ATTN: R D SENO

FORD AEROSPACE & COMMUNICATIONS CORP
    ATTN: PRESIDENT

G B LABORATORY, INC
    ATTN: G BURGHART

GENERAL RESEARCH CORP
    ATTN: E STEELE
    ATTN: R GLOBUS

GEO CENTERS, INC
    ATTN: E MARRAM
    ATTN: H LINNERUD

GEOSCIENCE LTD
    ATTN: DR H POPPENDIEK

H-TECH LABS, INC
    ATTN: B HARTENBAUM

HTL K WEST
    ATTN: A D GOEDEKE

IIT RESEARCH INSTITUTE
    ATTN: DIRECTOR

JAYCOR
    ATTN: R STAHL

JAYCOR
    ATTN: R BONN

JAYCOR
    ATTN: PRESIDENT

KAMAN SCIENCES CORP
    ATTN: B TAYLOR
    ATTN: C HUDSON
    ATTN: D ELDER
    ATTN: D OSBORN
    ATTN: E COLE
    ATTN: F RICH
    ATTN: G ROARK
    ATTN: N KOOZER

KAMAN SCIENCES CORP
    ATTN: E CONRAD

LOS ALAMOS TECHNICAL ASSOCIATES, INC
    ATTN: PRESIDENT

M I T LINCOLN LAB
    ATTN: DR R SLATTERY

MITRE CORP
    ATTN: J E DRIVER

NEW MEXICO ENGINEERING RESEARCH INSTITUTE
    ATTN: DIRECTOR

PACIFIC-SIERRA RESEARCH CORP
    ATTN: H BRODE, CHAIRMAN SAGE
    ATTN: R SMALL

PACIFIC-SIERRA RESEARCH CORP
    ATTN: G MCLELLAN

PACIFICA TECHNOLOGY
    ATTN: R ALLEN

PHYSICAL DYNAMICS, INC
    ATTN: B KREISS

PHYSICS APPLICATIONS, INC
    ATTN: DOCUMENT CONTROL

PHYSICS INTERNATIONAL CO
    ATTN: G MANKINEN
    ATTN: P CAYERE
    ATTN: R Z CONROW

R & D ASSOCIATES
    ATTN: C K B LEE
    ATTN: D HOLLIDAY
    ATTN: D SIMONS
    ATTN: F A FIELD
    ATTN: J LEWIS

RAND CORP
    ATTN: P DAVIS

RAND CORP
    ATTN: B BENNETT

DEPT OF DEFENSE CONTRACTORS (CONTINUED)

RAYTHEON CO
    ATTN: J WECKBACK

RIVERSIDE RESEARCH INSTITUTE
    ATTN: PRESIDENT

S-CUBED
    ATTN: C PETERSEN
    ATTN: D GRINE
    ATTN: P COLEMAN

SCIENCE & ENGRG ASSOCIATES, INC
    ATTN: J CRAMER

SCIENCE & ENGRG ASSOCIATES, INC
    ATTN: J STOCKTON
    ATTN: R BEATY

SCIENCE APPLICATIONS INTL CORP
    ATTN: K SITES
    ATTN: L A MILLONZI

SCIENCE APPLICATIONS INTL CORP
    ATTN: L SCOTT
    ATTN: R SCHLAUG

SCIENCE APPLICATIONS INTL CORP
    ATTN: B GORDON
    ATTN: E TOTON
    ATTN: S METH

SCIENCE APPLICATIONS INTL CORP
    ATTN: V J ORPHAN

SRI INTERNATIONAL
    ATTN: D KEOUGH
    ATTN: E VANCE
2 CYS ATTN: J AIDUN
    ATTN: P DE CARLI

TELEDYNE BROWN ENGINEERING
    ATTN: PRESIDENT

WASHINGTON STATE UNIVERSITY
    ATTN: PROF G DUVALL
    ATTN: PROF Y GUPTA

FOREIGN

ATOMIC WEAPONS RESEARCH ESTABLISHMENT
    ATTN: J BALDERSTON

AUSTRALIA EMBASSY
    ATTN: OFC OF THE DEF SCI ATTACHE

BRITISH DEFENCE STAFF
    ATTN: ACOW S MITCHELL

DEFENSE RESEARCH ESTABLISHMENT
    ATTN: DR J ANDERSON
    ATTN: I MOEN

DEFENSE TECH & PROCUREMENT GROUP
    ATTN: B ANET

ERNST-MACH-INSTITUT
    ATTN: H REICHENBACH

FEDERAL INSTITUTE OF TECHNOLOGY
    ATTN: DR J STUDER

ISRAEL EMBASSY
    ATTN: OFC OF THE MIL ATTACHE

NATIONAL DEFENCE RESEARCH INSTITUTE
    ATTN: H AXELSSON
    ATTN: H GORAN

NORWEGIAN EMBASSY
    ATTN: MILITARY ATTACHE

ROYAL NETHERLANDS EMBASSY
    ATTN: MILITARY ATTACHE

SWEDISH EMBASSY
    ATTN: ASSISTANT ARMY ATTACHE

TECHNOLOGISCH LABORATORIUM (TNO)
    ATTN: DIRECTOR

END

11-86

DTIC